



Cite this: *Soft Matter*, 2024, 20, 2926

# Phenylboronate-salicylate ester cross-linked self-healing hydrogel composed of modified hyaluronan at physiological pH†

Ryotaro Miki, \* Tsutomu Yamaki, Masaki Uchida and Hideshi Natsume

Several hydrogels with boronate/diol ester cross-linking have been reported. However, multiple synthetic steps or expensive reagents are required to modify some diol moieties into polymers. Therefore, diol-modified polymers, which are easily and inexpensively prepared via a single-step process, are required for the formation of boronate esters. This study reports a novel hydrogel composed of phenylboronic acid-modified hyaluronic acid and salicylic acid-modified hyaluronic acid. This hydrogel is injectable, can self-heal at physiological pH, and can be easily and inexpensively prepared. The polymer system behaved as a sol at pH 12.0 and a weak gel at pH 9.4 and 11.2, whereas it behaved as a gel over a wide pH range of 4.0–8.2. The viscoelasticity of the system decreased in response to sugar at pH 7.3. Thus, salicylic acid can be considered a promising diol moiety for hydrogel formation via boronate ester cross-linking.

Received 23rd October 2023,  
Accepted 27th February 2024

DOI: 10.1039/d3sm01417g

rsc.li/soft-matter-journal

## Introduction

Over the past decade, hydrogels have attracted considerable attention because of their potential applications in various fields, including in drug delivery systems,<sup>1</sup> regenerative medicine,<sup>2</sup> and wound dressings.<sup>3</sup> In particular, when self-healing hydrogels are extruded from a syringe, they quickly return to the gel state. This property renders them attractive for clinical applications as they can be surgically implanted in patients in a minimally invasive manner.<sup>1</sup> Moreover, dynamic covalent cross-linking, such as boronate/diol esters, imine bonds, and disulfide bonds, may be utilised to endow hydrogels with self-healing ability.<sup>4</sup>

Phenylboronic acid (PBA) is a type of Lewis acid; at a pH higher than its  $pK_a$  ( $K_a$ : acid dissociation constant), the hydroxyl group is coordinated to PBA, resulting in an increase in the concentration of the negatively charged ionic form. This elevated concentration enables PBA to reversibly form cyclic esters with *cis*-diol compounds such as sugars (Fig. 1a).<sup>5</sup> The degree of boronate/diol ester bonding depends on the binding constant between the boronic acid and diol compounds.<sup>6</sup> Numerous flexible hydrogels formed *via* boronate/diol ester cross-linking under physiological pH conditions have been developed till now.<sup>7–15</sup> In particular, injectable hydrogels based on boronate esters have good potential in clinical applications.<sup>16,17</sup> For

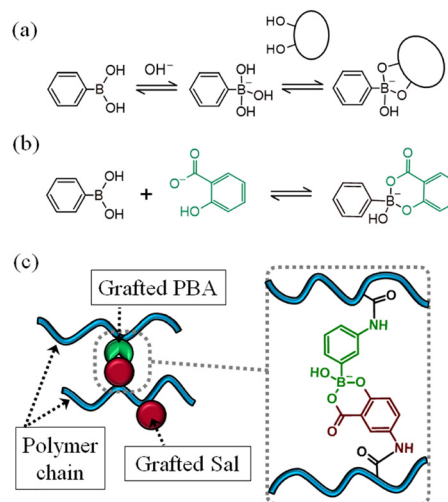


Fig. 1 (a) Acid–base equilibrium of PBA, and the binding equilibrium between PBA and a *cis*-diol. (b) Reaction scheme of phenylboronate/salicylate ester formation. (c) Schematic of the cross-linking of the PBA-modified and Sal-modified polymer system.

instance, the hydrogel formed using boronate esters exhibited effectiveness in the treatment of brain lesions in small animal models.<sup>16</sup> These findings suggest that the hydrogel facilitates neuronal infiltration and closure of lesions while serving a viscoelastic function, mimicking the extracellular matrix in brain injury healing. In the boronate-ester-cross-linked hydrogels, diol moieties, such as catechol,<sup>7,8</sup> sugar,<sup>9–13</sup> and salicyl-hydroxamic acid,<sup>14,15</sup> are modified to the partner polymer of

Faculty of Pharmacy and Pharmaceutical Sciences, Josai University, 1-1 Keyakidai, Sakado, Saitama 350-0295, Japan. E-mail: rmiki@josai.ac.jp; Fax: +81-49-271-7052; Tel: +81-49-271-7052

† Electronic supplementary information (ESI) available. See DOI: <https://doi.org/10.1039/d3sm01417g>



the boronic-acid-modified polymer. For example, catechol,<sup>6</sup> fructose,<sup>12</sup> and D-gluconolactone<sup>10</sup> derivatives exhibit high binding constants with boronic acid moieties; thus, they are applicable in the preparation of hydrogels wherein boronate esters serve as cross-linking sites. However, these diol moieties are unsuitable for practical applications and large-scale synthesis for the following reasons. Polyphenols, such as catechol, are easily oxidised; therefore, their proper storage is essential to ensure stability.<sup>18,19</sup> Salicylhydroxamic acid is a promising diol moiety to bind with PBA;<sup>20,21</sup> a polymer with the salicylhydroxamic acid moiety can form a hydrogel *via* boronate ester cross-linking through PBA-polymer composite formation even at a pH lower than the  $pK_a$  of the standard PBA derivative ( $pK_a$  8–9).<sup>14,15</sup> However, multiple synthetic steps are required to modify salicylhydroxamic acid into a polymer.<sup>14,15</sup> A multi-step synthesis is typically more time-consuming than one-step routes, impeding the synthesis of diol-modified polymers on a commercial scale and limiting their practical applications. Although D-gluconolactone can be modified to aminated polyethylene glycol (PEG) during one-step synthesis, this synthesis cannot be conducted on a large scale because of the requirement of expensive aminated PEG.<sup>10,11</sup> Amino sugars such as fructosamine can be easily modified into polymers with carboxyl groups in a single step.<sup>9,12,13</sup> However, some amino sugars including fructosamine are too expensive to be utilised in the synthesis of diol-modified polymers on a practical scale. Therefore, diol-modified polymers for the formation of boronate esters are required that can be easily and inexpensively prepared in one step. Boric acid and PBAs reversibly form ester bonds with salicylates (Sal) (Fig. 1b).<sup>22,23</sup> Therefore, hydrogels can be prepared by combining PBA-modified and Sal-modified polymers (Fig. 1c). However, to the best of our knowledge, such polymeric materials have not yet been reported.

Hyaluronic acid (HA) is a biodegradable and highly biocompatible nonsulphated glycosaminoglycan. It has been extensively studied as a base polymer for hydrogels and is expected to be applied in drug delivery systems,<sup>24</sup> tissue engineering,<sup>25</sup> and skin-wound healing.<sup>26</sup> PBA-moieties modified HAs have also been reported, and a hydrogel is produced by self-crosslinking a PBA moiety with the diol of HA.<sup>27–30</sup> However, PBA-moieties modified HAs also have some limitations. Although standard PBA derivatives can be modified to HA using a single step synthesis method, a hydrogel is formed only under the basic condition (pH 9.2–10.5).<sup>27–29</sup> Some benzoxaborole derivatives-modified HA can form hydrogels under physiological pH conditions.<sup>30</sup> However, multi-step syntheses are required to synthesize benzoxaborole derivatives.

In this study, a novel hydrogel composed of PBA-modified HA and Sal-modified HA is reported. This hydrogel is injectable, can self-heal at physiological pH, and can be easily and inexpensively prepared.

## Experimental section

### Materials and methods

D-Glucose (Glc), D-fructose (Fru), sodium salicylate (NaSal), alizarin red S (ARS), hydrochloric acid (5 mol L<sup>−1</sup>), sodium

hydroxide (NaOH) solution (8 mol L<sup>−1</sup>), disodium hydrogen phosphate, sodium dihydrogen phosphate, *N,N*-dimethylformamide (DMF), and dimethyl sulfoxide (DMSO) were obtained from FUJIFILM Wako Pure Chemical Co. (Osaka, Japan). Furthermore, 3-acetamidophenylboronic acid (3AcAmBA) was purchased from Nacalai Tesque Inc. (Tokyo, Japan), whereas sodium hyaluronate (NaHA, 50–110 kDa) was purchased from Kikkoman Biochemistry (Tokyo, Japan). Additionally, 3-aminophenylboronic acid (3APBA) monohydrate, 5-aminosalicylic acid (ASal), fluorescein sodium salt (Flu), and bromophenol blue (BPB) were obtained from Tokyo Chemical Industry (Tokyo, Japan). Deuterium oxide (D<sub>2</sub>O) was obtained from Kanto Chemical Co., Inc. (Tokyo, Japan); sodium deuteroxide (NaOD) solution (40% w/w) and 4-(4,6-dimethoxy-1,3,5-triazin-2-yl)-4-methylmorpholinium chloride (DMT-MM) were purchased from Sigma-Aldrich (Tokyo, Japan). 3-(4,5-Dimethylthiazol-2-yl)-2,5-diphenyltetrazolium bromide (MTT), a tetrazolium dye, was obtained from Dojin Chemical Co. (Kumamoto, Japan). Human lung adenocarcinoma (A549) cell lines were obtained from Riken Cell Bank (Ibaraki, Japan). Dulbecco's modified Eagle medium (DMEM) and fetal bovine serum (FBS) were purchased from Thermo Fisher Scientific (Waltham, MA, USA). Finally, cellulose tubes (36/32; molecular weight cutoff: 14 kDa) were acquired from Viskase Companies, Inc. (IL, USA).

### Synthesis of PBA-modified HA (BA-HA)

BA-HA was synthesised using a slightly modified previous method.<sup>27</sup> Briefly, 3APBA (62.0 mg, 400 μmol) was added to distilled water (70 mL) and ultrasonically dissolved. Subsequently, NaHA (1043.2 mg, 2.50 mmol as repeating units) was dissolved in the mixture, after which DMT-MM (166.0 mg, 600 μmol) was added, and the pH of the solution was adjusted to 6.5 using hydrochloric acid. A turbid reaction mixture was obtained after stirring for 24 h at room temperature. Next, an adequate amount of 8 M NaOH was added to ensure complete dissolution. Finally, the reaction solution was dialysed against water in a cellulose tube and freeze-dried.

### Synthesis of salicylate-modified HA (Sal-HA)

Sal-HA was synthesised *via* a condensation reaction. Briefly, ASal (160.1 mg, 1.25 mmol) was added to DMF (25 mL) and dissolved ultrasonically. Next, NaHA (1043.2 mg, 2.50 mmol as repeating units) was dissolved in distilled water (60 mL). The ASal solution (25 mL) was subsequently added to the NaHA aqueous solution (60 mL), followed by the addition of DMT-MM (518.8 mg, 1.88 mmol); the pH of the solution was adjusted to 5.5 using the NaOH solution. The mixture was allowed to react for 24 h at room temperature. To avoid the precipitation of ASal during dialysis, an adequate amount of 8 M NaOH was added. Finally, the reaction solution was dialysed against water in a cellulose tube and freeze-dried.

### <sup>1</sup>H NMR analysis

<sup>1</sup>H nuclear magnetic resonance (NMR) spectroscopy was performed using a 600 MHz Bruker AVANCE NEO 600 spectrometer (Bruker Japan KK, Kanagawa, Japan). D<sub>2</sub>O was used as



the solvent for preparing the samples for the analysis of modified polymers and 3APBA, whereas the 0.3 M NaOD/D<sub>2</sub>O solution was used for ASal.

The HDO solvent peak (4.63 ppm) was used as a chemical shift reference. The degree of substitution was determined by calculating the ratio of the integrated phenyl proton signals originating from 3APBA (7.3–8.0 ppm,  $-\text{C}_6\text{H}_4$ ) or ASal (6.8–8.0 ppm,  $-\text{C}_6\text{H}_3$ ) to signals of the HA methyl protons (1.4 and 1.9 ppm,  $-\text{CH}_3$ ).

### Preparation of BA–HA/Sal–HA systems

The BA–HA/Sal–HA systems consist of 16.0 mg mL<sup>−1</sup> BA–HA and 16.0 mg mL<sup>−1</sup> Sal–HA (1:1 wt%), except for the part of rheological studies and the *in vitro* biocompatibility test. Phosphate buffers (0.20 M, pH 3.4–12.4) were used as solvents. To investigate the influence of Fru and Glc, 0.20 M phosphate buffer (pH 7.4) was used as a solvent. Note that the prepared samples (1.02 mL or 170  $\mu\text{L}$ ) were stored at 25 °C for more than 24 h prior to use. To observe the injection and self-healing property of the BA–HA/Sal–HA systems, samples containing 50  $\mu\text{M}$  BPB or 300  $\mu\text{M}$  Flu were prepared. For injectability testing, a 30 G injection needle (outer diameter: 0.31 mm; inner diameter: 0.13 mm) was used. The pH of the BA–HA/Sal–HA systems was measured using a pH meter (LAQUA act D71, Horiba Ltd, Kyoto, Japan) with a flat ISFET electrode (0040-10D, Horiba Ltd).

### Dynamic rheological measurements

Dynamic rheological measurements were performed using a stress-controlled rotational rheometer (MCR-102, Anton Paar, Ostfildern, Germany) with a solvent trap and cone plate at 25 °C. An oscillatory strain-sweep study was conducted, wherein strains of 0.1–1000% were applied at a frequency of 2 rad s<sup>−1</sup>. An oscillatory step-strain study was performed by repeating a low strain (1%, 1 min) for healing and a high strain (400%, 1 min) for breaking. Frequency-sweep studies were performed at a fixed strain of 10%. A 170  $\mu\text{L}$  cone-plate load-volume was applied to the rheometer stage.

### Scanning electron microscopy (SEM)

The BA–HA/Sal–HA systems (8–12 mg) prepared using a 0.20 M phosphate buffer (pH 3.4, 7.4, and 11.4) were placed in a microtube and immersed into cold ethanol (−80 °C), followed by rapid freezing. Thereafter, the samples were stored in a deep freezer at −80 °C for more than 24 h and thoroughly lyophilised. All samples were coated *via* Pt sputtering to increase their conductivity. Field-emission scanning electron microscopy (FE-SEM) was performed using a field-emission scanning electron microscope (JSM-IT800 SHL, JEOL Ltd, Tokyo, Japan).

### Fluorescence measurements for the determination of apparent binding constant

Fluorescence spectra were recorded on an Infinite 200 Pro M Nano+ microplate reader (Tecan Japan Co., Ltd, Kanagawa, Japan) with an excitation wavelength of 468 nm and an emission wavelength of 572 nm. The solutions containing 9.0  $\mu\text{M}$

ARS and 2.0 mM 3AcAmBA were prepared using 0.10 M phosphate buffers (pH 5.4–9.4). Diol compound stock solutions were prepared using an ARS/3AcAmBA solution as a solvent. Samples were prepared by mixing the respective stock solutions. The apparent binding constants ( $K$ ) between 3AcAmBA and the diol compounds were determined according to a previously reported method.<sup>31,32</sup>

### Ultraviolet (UV) spectroscopy

An ultraviolet (UV) spectrophotometer (UVmini-1240, Shimadzu, Kyoto, Japan) was used for the determination of  $pK_a$  values and analysis of modified HA. For the determination of the  $pK_a$  values, absorbance spectra were recorded for BA–HA (0.10 mM PBA moiety, 1.03 mM HA repeating units), 1.0 mM 3AcAmBA, and Sal–HA (0.24 mM Sal moiety, 0.90 mM HA repeating units) in distilled water. For absorbance measurement, hydrochloric acid or NaOH solution was used to adjust the pH. For hydrogel stability testing, the UV spectra of modified HA in the 0.20 M phosphate buffer (pH 7.4) were recorded.

### Hydrogel stability testing

To evaluate the stability of the BA–HA/Sal–HA hydrogel under physiological conditions, the dissolution of the BA–HA/Sal–HA system in a bulk phosphate buffer (0.20 M, pH 7.4) at 37 °C was investigated. The BA–HA/Sal–HA system (170  $\mu\text{L}$ , pH 7.3) with the phosphate buffer (0.20 M, pH 7.4) was placed in a 1.5 mL microtube. After centrifugation, the samples were stored at 37 °C for more than 24 h. Before the start of the testing, 680  $\mu\text{L}$  of phosphate buffer (0.20 M, pH 7.4), prewarmed to 37 °C, was gently added to the microtubes. The microtubes were gently shaken 10 times before sampling 400  $\mu\text{L}$  of the bulk aqueous solution with time. Subsequently, the microtubes were refilled with 400  $\mu\text{L}$  of the fresh prewarmed phosphate buffer. The absorbance of the sampled solution was measured at 320 nm using a microplate reader (Infinite 200 Pro M Nano+ microplate reader). A calibration curve was generated on the basis of absorbance measurements at 320 nm using a solution containing Sal–HA and BA–HA (1:1 wt%) with a phosphate buffer (0.20 M, pH 7.4).

### *In vitro* biocompatibility test

Before biocompatibility testing, A549 cells were seeded in a 48-well plate at a density of  $1.0 \times 10^5$  cells per cm<sup>2</sup> in DMEM supplemented with 10% FBS, incubated at 37 °C in a humidified atmosphere of 5% CO<sub>2</sub>, and cultured to be about 90% confluence. Native HA or modified HA was dissolved (2.0 mg mL<sup>−1</sup>) in DMEM and added to each cell, followed by 24 h of incubation. As a control, cells were incubated only in growth media. After 24 h of incubation, the medium was replaced with DMEM containing MTT (0.5 mg mL<sup>−1</sup>), and the cells were incubated for 3 h at 37 °C. After removing the medium, DMSO was added to each well to dissolve the resulting formazan. The absorbance of the solution was measured at a wavelength of 530 nm using a microplate reader (Infinite 200 Pro M Nano+ microplate reader). The cell viability was expressed as a percentage of



absorbance of the polymer (native HA or modified HA)-treated cells to that of the untreated cells.

## Results and discussion

### Synthesis of BA-HA and Sal-HA

BA-HA and Sal-HA were synthesised *via* condensation reactions between the amino groups of 3APBA or ASal and the carboxyl groups of HA (Fig. 2a and b). The BA-HA solution was transparent and pale yellow-green before the reaction; however, it became cloudy after 24 h of reaction (Fig. 2c). The turbid solution turned clear upon adding an appropriate amount of NaOH (image not shown). Generally, because the PBA-moiety-modified polymer has low solubility at a pH lower than the  $pK_a$  of the PBA moiety, it is inferred that turbidity was induced by BA-HA. The Sal-HA solution was transparent orange before and after the reaction (Fig. 2d). The freeze-dried BA-HA and Sal-HA samples were white and light pink spongy, respectively (Fig. 2e and f). To estimate the degree of substitution of the amino compounds to HA, the  $^1\text{H}$  NMR spectrum of each amino compound was recorded. The peaks ascribed to the benzene ring appeared at 6.8–7.2 and 6.5–6.9 ppm in 3APBA and ASal, respectively (Fig. S1, ESI $^\dagger$ ). In BA-HA and Sal-HA, the peaks associated with the benzene rings were observed at 7.3–8.0 ppm and 6.8–8.0 ppm, respectively (Fig. 3a and b). Moreover, the peaks attributed to the acetyl groups were observed at 1.4 and 1.9 ppm. The degree of substitution of the amino compounds was determined *via*  $^1\text{H}$  NMR analysis. The boronic acid and Sal

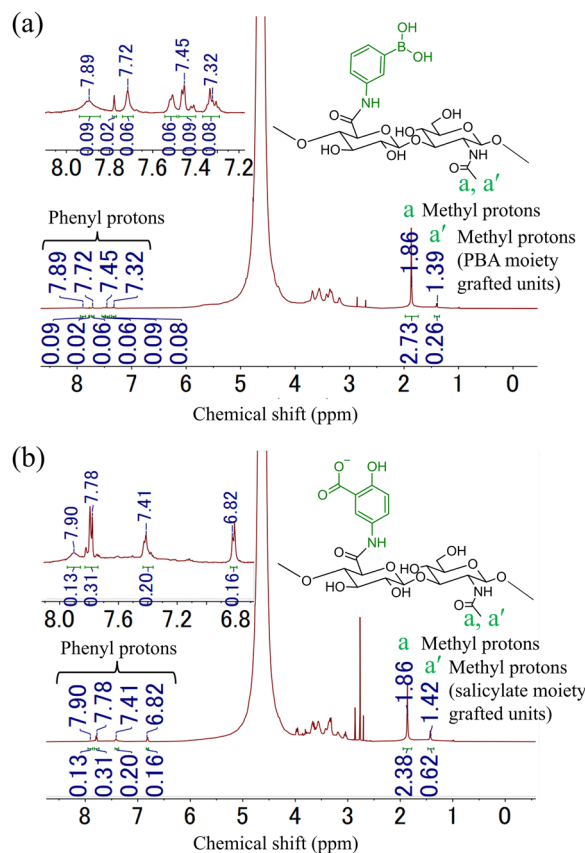


Fig. 3  $^1\text{H}$  NMR spectra of (a) BA-HA, and (b) Sal-HA.

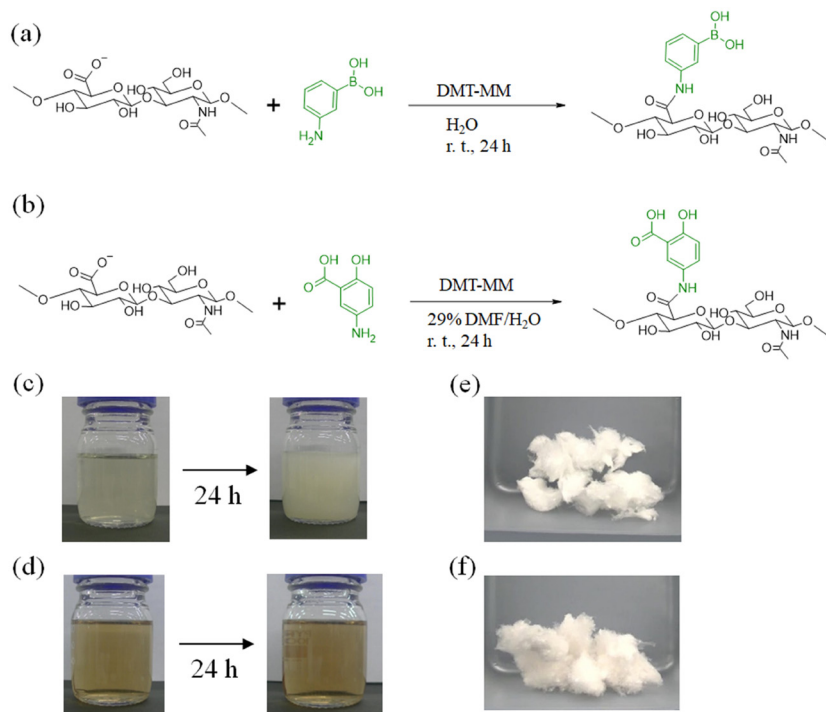


Fig. 2 Synthesis scheme of (a) BA-HA, and (b) Sal-HA. Images of the reaction solution before and after the synthesis of (c) BA-HA and (d) Sal-HA. Images after freeze drying of (e) BA-HA and (f) Sal-HA.



moieties were modified to the repeating units of HA by 10.0% and 26.7%, respectively.

### Visual appearance

Given that pH influences the formation of ester bonds between PBA derivatives and diol compounds,<sup>6</sup> the pH dependence of the BA-HA/Sal-HA system was investigated. It has been suggested that the phosphate buffer affects the affinity between PBA and ARS (a catechol dye), whereas it does not significantly affect the affinity between PBA and Fru.<sup>6</sup> In addition, the phosphate assists viscoelastic properties of boronate-ester-cross-linked hydrogels.<sup>33</sup> In order to eliminate the influence of buffer salts on viscoelasticity, the pH buffer in this study was unified to the phosphate buffer. The pH of each sample was slightly different from the pH of the solvent buffer. The samples were prepared over a wide pH range of 4.0–12.0 (Fig. 4a). Evidently, the samples at pH 4.0–8.2 almost did not flow after inverting the vial, behaving like a gel. In contrast, the samples at pH 9.4 and 11.2 flowed slowly, behaving like a viscous solution. The samples at pH 12.0 flowed quickly, acting like a sol. Note that when diol compounds are added to a polymer gel cross-linked by a boronate/diol ester, the cross-links are competitively cleaved, and the polymer gel becomes a sol. To confirm the sugar responsiveness of the boronate-ester-cross-linked hydrogels, the samples containing Glc and Fru were observed at pH 7.3. Both samples with 400 mM Glc and 40 mM Fru flowed more quickly than those without sugar at pH 7.3 (Fig. 4b). These results indicate that the BA-HA/Sal-HA system became a sol in response to sugar.

The injectability and self-healing ability of the boronate-ester-cross-linked hydrogels were evaluated for the practical applications.<sup>12,28,34</sup> The injectability and self-healing ability of the BA-HA/Sal-HA system (pH 7.3) were studied through staining for easy observation. The BA-HA/Sal-HA system could be injected using a 30 G injection needle (Fig. 5a and Movie S1, ESI†). Furthermore, each BA-HA/Sal-HA gel piece, stained purple/yellow-green, respectively, could be stretched from both sides after contact for a few seconds (Fig. 5b and Movie S2, ESI†).

### Dynamic viscoelasticity measurements

For quantitatively evaluating the two crucial properties of self-healing hydrogels, namely, gelation and viscosity, dynamic viscoelasticity measurement is a widely used method.<sup>12,13,27–30,35</sup>

The dynamic viscoelastic properties of BA-HA/Sal-HA were investigated. The storage modulus ( $G'$ ) and loss modulus ( $G''$ ) were obtained from the dynamic viscoelasticity measurements, which showed the solid and liquid properties, respectively. Oscillatory strain-sweep measurements were performed to investigate the strain at which the gel broke (Fig. 6a). The  $G'$  value of the BA-HA/Sal-HA system remained constant (684–712 Pa) at 0.1% to 147% strain, whereas it began to decrease at 164% strain (686 Pa). This indicates that the gel broke down at a strain of 160%. Oscillatory strain-step measurements were performed to investigate the self-healing ability of the hydrogel (Fig. 6b). At a low strain (1%), the  $G'$  and  $G''$  values remained constant (775–783 Pa and 317–318 Pa, respectively), thus indicating that the gel property was stronger. In contrast, at a high strain (400%), the  $G'$  and  $G''$  values decreased to 122 Pa and 261 Pa, respectively,

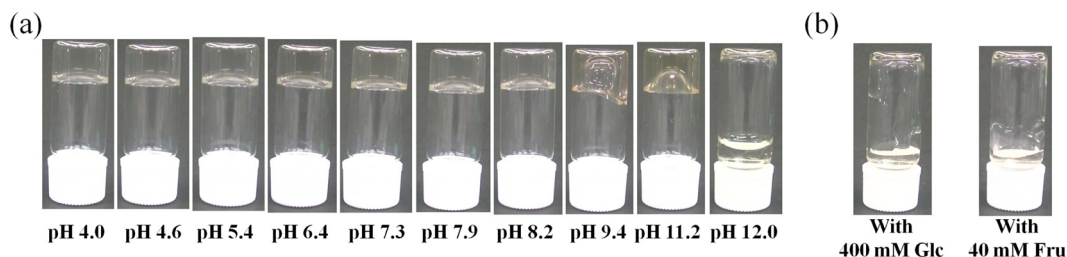


Fig. 4 Visual observation of  $16.0 \text{ mg mL}^{-1}$  BA-HA/ $16.0 \text{ mg mL}^{-1}$  Sal-HA system in (a) 0.20 M phosphate buffers at different pH values and (b) the 0.20 M phosphate buffer at pH 7.4 with sugars. Images were taken 20 s after inverting the vials.

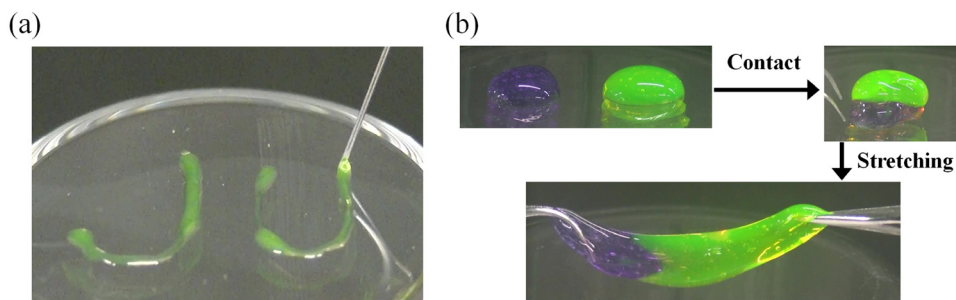


Fig. 5 Images showing the (a) injectability of the BA-HA/Sal-HA system using a 30 G injection needle, and (b) self-healing ability of the  $16.0 \text{ mg mL}^{-1}$  BA-HA and  $16.0 \text{ mg mL}^{-1}$  Sal-HA systems at pH 7.3.



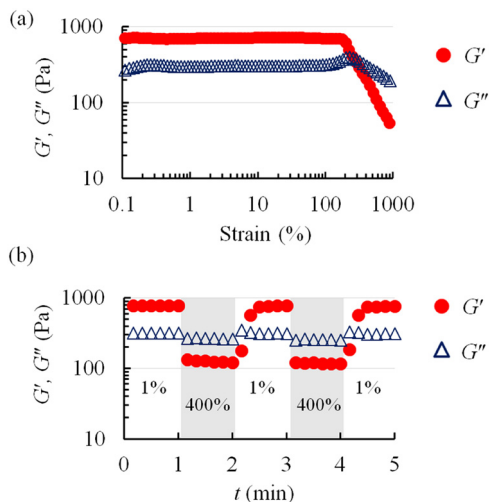


Fig. 6 (a) Oscillatory strain-sweep and (b) oscillatory step-strain studies of the  $16.0 \text{ mg mL}^{-1}$  BA-HA and  $16.0 \text{ mg mL}^{-1}$  Sal-HA system at pH 7.3.

indicating that the sol property was stronger. Subsequently, when the strain was reduced, the  $G'$  value quickly recovered to 770 Pa (recovery rate: 98.3%), demonstrating the self-healing ability of the system.

The  $G'$  and  $G''$  values of boronate-ester-cross-linked hydrogels are strongly frequency ( $\omega$ ) dependent.<sup>12,13,27–30,35</sup> The frequency dependence of the BA-HA/Sal-HA system was investigated at a fixed strain of 10% (Fig. 7a). The BA-HA/Sal-HA

system at pH 5.4 and 7.3 demonstrated similar frequency-dependent dynamic viscoelastic profiles. The  $G'$  value of the BA-HA/Sal-HA system at pH 5.4, 7.3, and 11.2 was lower than the  $G''$  value in the low-frequency range but higher at above 0.80, 0.63 and 0.57  $\text{rad s}^{-1}$ , respectively. The  $G'$  value at pH 11.2 was much lower than that at pH 7.3 at all frequencies.

The pH dependency of  $G'$  and  $G''$  in the BA-HA/Sal-HA system at  $10 \text{ rad s}^{-1}$  was investigated (Fig. 7b). The  $G'$  values were similar (minimum: 460 Pa at pH 5.4, maximum: 816 Pa at pH 7.3) at pH 4.0–7.3. At pH > 7.3, the  $G'$  value decreased to 52.3 Pa upon increasing the pH to 11.2. At pH 12.0, the  $G'$  and  $G''$  values could not be obtained because the viscoelasticity was too low for accurate measurement. At pH 4.0–8.2, the  $G'$  value was much higher than the  $G''$  value, indicating that the gel property was stronger. It is interesting that the BA-HA/Sal-HA system exhibited a strong gel property over a wide pH range—from acidic to slightly alkaline (pH 4.0–8.2). The hydrogels formed *via* boronate ester cross-linking between salicylhydroxamic acid and PBA also exhibited a strong gel property at pH 4.2 and 7.6.<sup>14</sup> Although the hydrogels formed *via* the cross-linking of the boronate ester composed of Fru-modified HA<sup>12</sup> or maltose-modified HA<sup>35</sup> exhibited a high  $G'$  value at pH 7–9, the  $G'$  value drastically decreased at pH 6. Therefore, the salicylic acid moiety imparted a pH dependence different from that of sugars such as Fru and maltose as the diol moiety of the partner polymer that forms the hydrogel *via* boronate ester

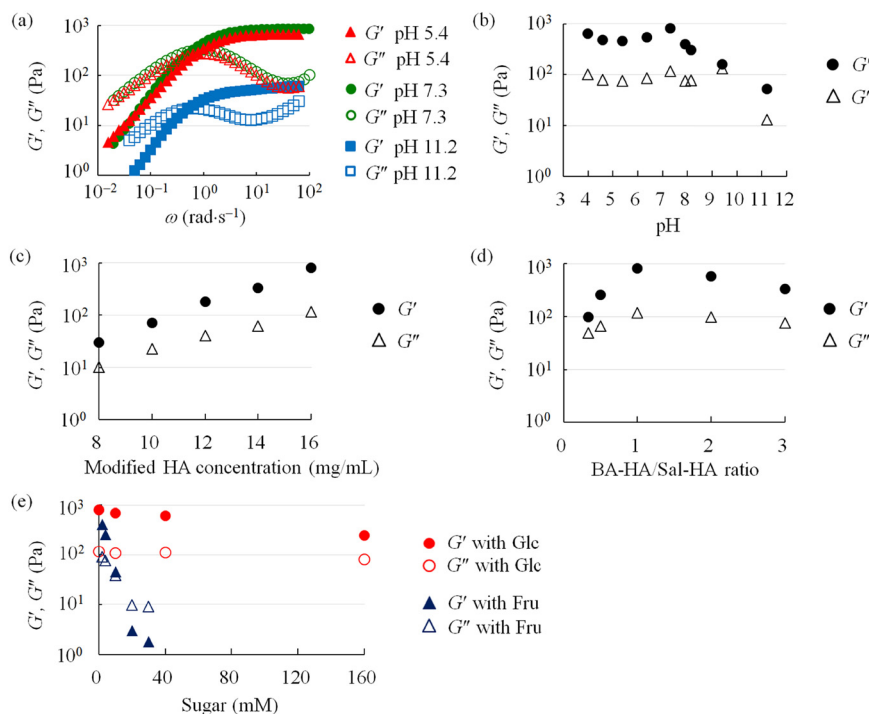


Fig. 7 (a) Frequency-sweep study of the  $16.0 \text{ mg mL}^{-1}$  BA-HA and  $16.0 \text{ mg mL}^{-1}$  Sal-HA system. (b)–(e) Profiles of  $G'$  or  $G''$  at  $10 \text{ rad s}^{-1}$  plotted for the BA-HA/Sal-HA system. (b) Profiles of  $G'$  or  $G''$  as a function of pH for the  $16.0 \text{ mg mL}^{-1}$  BA-HA and  $16.0 \text{ mg mL}^{-1}$  Sal-HA systems at pH 7.3. (c) Profiles of  $G'$  or  $G''$  as a function of concentration of BA-HA and Sal-HA (1:1 wt%) at pH 7.3. (d) Profiles of  $G'$  or  $G''$  as a function of the concentration ratio of BA-HA/Sal-HA at pH 7.3 (total modified HA concentration was fixed at  $32.0 \text{ mg mL}^{-1}$ ). (e) Profiles of  $G'$  or  $G''$  as a function of sugar concentrations in the  $16.0 \text{ mg mL}^{-1}$  BA-HA and  $16.0 \text{ mg mL}^{-1}$  Sal-HA systems at pH 7.3.



cross-linking. The boronic acid moiety also forms dynamic ester bonds with the diol of HA under the basic condition (pH 9.2–10.5).<sup>27–29</sup> In this study, the degree of substitution of boronic acid was 10.0%, which is excessively low to form a gel *via* the cross-linking of a boronate ester between boronic acid and the diol of HA. Thus, even at pH 11.2, the boronate ester between boronic acid and the diol of HA did not significantly affect the  $G'$  value of the BA–HA/Sal–HA system (Fig. 7b).

Because the polymer concentration has a strong effect on viscoelasticity, the influence of the polymer concentration was investigated in boronate-ester-cross-linked hydrogels.<sup>9,10,35,36</sup> The modified HA concentration dependency of the  $G'$  and  $G''$  values at 10 rad s<sup>−1</sup> was investigated in the BA–HA/Sal–HA system (1:1 wt%) at pH 7.3 (Fig. 7c). The  $G'$  value was higher than the  $G''$  value at all modified HA concentrations (8.0–16.0 mg mL<sup>−1</sup>), indicating that the BA–HA/Sal–HA system has a stronger gel property than the sol property. The  $G'$  and  $G''$  values were the lowest (29.7 Pa and 10.2 Pa, respectively) in the 8.0 mg mL<sup>−1</sup> BA–HA and 8.0 mg mL<sup>−1</sup> Sal–HA system and increased in a concentration-dependent manner.

Because the composition of the two cross-linked polymers considerably affects the viscoelasticity of the boronate-ester-cross-linked hydrogels, the influence of the composition of the polymers was investigated.<sup>7,9,36</sup> The effect of the concentration ratio of BA–HA/Sal–HA on the  $G'$  and  $G''$  values at 10 rad s<sup>−1</sup> was investigated for the BA–HA/Sal–HA system at pH 7.3 (total modified HA concentration was fixed at 32.0 mg mL<sup>−1</sup>; Fig. 7d). The  $G'$  value was higher than the  $G''$  value at all concentration ratios of BA–HA/Sal–HA, indicating that the gel property was stronger. The  $G'$  and  $G''$  values were the lowest at the BA–HA/Sal–HA ratio of 0.33 (BA–HA : Sal–HA = 1 : 3) and the highest at a ratio of 1.0. At the ratio of 0.33, the difference between the  $G'$  and  $G''$  values was smaller than that at the ratio of 1.0; thus, the gel property was weaker than that at the ratio of 1.0. At the ratio of 3.0, the  $G'$  value slightly decreased from 816 to 335 Pa as the ratio increased >1.0. These results were reasonable to some extent because the degree of substitution of Sal–HA (26.7%) was higher than that of BA–HA (10.0%). For instance, the amount of the boronic acid moiety is too less to allow its binding with the Sal moiety at the ratio of 0.33, leading to a low  $G'$  value.

The boronate-ester-cross-linked hydrogels possess the sugar-responsive ability to transform into a sol; thus, their dynamic viscoelasticities were evaluated for application to sugar-responsive drug release.<sup>10,27,30,36,37</sup> The sugar concentration

dependency of the  $G'$  and  $G''$  values at 10 rad s<sup>−1</sup> was investigated for the BA–HA/Sal–HA system (Fig. 7e). The  $G'$  value decreased in a sugar-concentration-dependent manner for both Fru and Glc. The  $G'$  value decreased to 45.5 and 694 Pa at 10 mM Fru and 10 mM Glc, respectively, indicating that Fru addition is more effective in decreasing the  $G'$  value than Glc addition. The binding constant of Fru with PBA at pH 7.4 is 35 times higher than that of Glc (160 M<sup>−1</sup> and 4.6 M<sup>−1</sup>, respectively),<sup>6</sup> justifying the result that Fru addition more effectively decreases the  $G'$  values. Similar phenomena have been reported in other boronate-ester-cross-linked hydrogels.<sup>30</sup> It is necessary to incorporate a PBA derivative with a high binding constant to Glc into the polymer to allow response at clinical Glc concentrations (5.5–22 mM).<sup>10</sup>

## SEM results

The SEM images of the freeze-dried hydrogels support the evidence of the three-dimensional cross-linking of boronate esters.<sup>7,8,28,38,39</sup> The porous structures on the micrometre order are typically observed in the freeze-dried hydrogels. The freeze-dried samples of the BA–HA/Sal–HA system at pH 4.0, 7.3, and 11.2 were observed through FE-SEM (Fig. 8). Clear micrometre-sized pores were observed in all samples at pH 4.0, 7.3, and 11.2 (Fig. 8). These results suggest that cross-linking by the boronate ester occurs in the samples at pH 4.0, 7.3, and 11.2. Although these results are not quantitative, they partly support the viscoelasticity of the BA–HA/Sal–HA systems (Fig. 7b).

## Hydrogel stability testing

Evaluating the stability of hydrogels under physiological conditions is important for their practical applications. Generally, hydrogels cross-linked *via* dynamic covalent boronate esters are more unstable than gels cross-linked by covalent bonds. To investigate the stability of the BA–HA/Sal–HA systems under physiological conditions of pH 7.4 and 37 °C, dissolution testing was performed using the phosphate buffer at pH 7.4 as the bulk solution. Prior to testing the dissolution of modified HA, the UV spectra of BA–HA and Sal–HA were recorded (Fig. 9a). At 320 nm, the spectrum of 0.38 mg mL<sup>−1</sup> BA–HA showed almost no absorption peaks, whereas that of 0.38 mg mL<sup>−1</sup> Sal–HA demonstrated absorbance at 0.23. The mixture solution containing 0.38 mg mL<sup>−1</sup> BA–HA and 0.38 mg mL<sup>−1</sup> Sal–HA exhibited almost the same absorbance (Abs 0.24) as that of Sal–HA alone. The dissolution of Sal–HA from the BA–HA/Sal–HA hydrogel

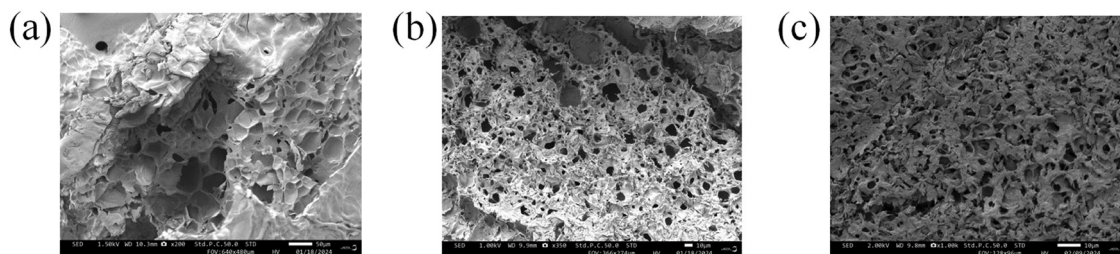


Fig. 8 FE-SEM images of the lyophilised BA–HA/Sal–HA systems at (a) pH 4.0, (b) pH 7.3, and (c) pH 11.2. The white scale bars at the bottom right of the images are (a) 50 µm, (b) 10 µm, and (c) 10 µm.



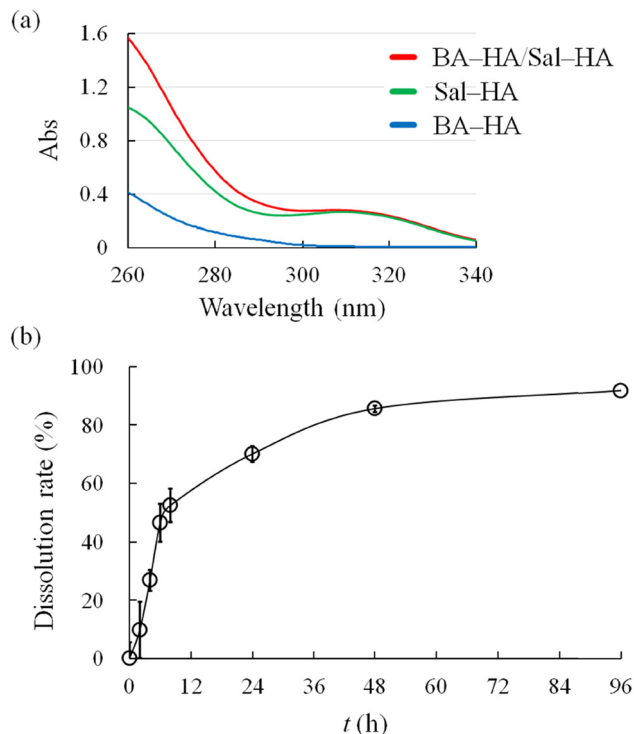


Fig. 9 (a) UV spectra of modified HA ( $0.38 \text{ mg mL}^{-1}$ ) at pH 7.4. (b) Dissolution profiles of modified HA from the BA-HA/Sal-HA system. The data represent the mean  $\pm$  standard deviation ( $n = 4$ ).

was quantified at 320 nm, and the dissolution rate was calculated with time (Fig. 9b). We assumed that almost the same amount of BA-HA as that of Sal-HA would be eluted from the hydrogel. Modified HA was rapidly eluted up to 8 h, and the dissolution rate was  $52.4\% \pm 6.4\%$  at 8 h. After 8 h, the elution slowed down, and the dissolution rate reached  $91.8\% \pm 1.1\%$  at 96 h. These results indicate that most of the modified HA composed of the hydrogels was eluted. The hydrogels formed *via* cross-linking of the boronate ester between polyphenols (epigallocatechin gallate or tannic acid) and boronic-acid-modified polymers are stable for more than 2 months under similar physiological conditions.<sup>19</sup> It is difficult to simply compare these results with the previously reported values because the test conditions and judgement criteria for hydrogel dissolution testing are not standardised. Based on the results, it can be observed that the BA-HA/Sal-HA hydrogel at pH 7.3 is relatively unstable under physiological conditions. An additional cross-linking factor using other components is necessary for practical uses such as long-term *in vivo* implantation.

#### Determination of $pK_a$ and apparent binding constant

Given that the diol-binding properties of boronate esters are influenced by both the pH of the solution and  $pK_a$  of boronic acid and diol compounds,<sup>40</sup> the  $pK_a$  values of boronic acid in BA-HA, 3AcAmBA, and salicylic acid in Sal-HA were investigated through UV spectrophotometry (Fig. 10). Based on curve fitting between the absorbance and pH, the  $pK_a$  values of boronic acid in BA-HA, 3AcAmBA, and salicylic acid in Sal-HA

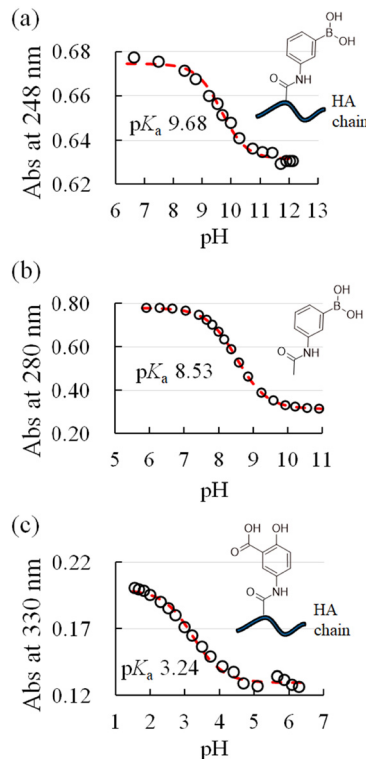


Fig. 10 Absorbance of (a) BA-HA (0.10 mM PBA moiety), (b) 3AcAmBA (1.0 mM), and (c) Sal-HA (0.24 mM Sal moiety) as a function of pH.

were calculated to be 9.68, 8.53, and 3.24, respectively. The  $pK_a$  of 3AcAmBA was reported to be 8.5;<sup>31</sup> thus, the obtained value is reasonable. Although the boronic acid of BA-HA is structurally similar to 3AcAmBA, a difference of approximately 1 in their  $pK_a$  values was observed. The  $pK_a$  value of salicylic acid in Sal-HA (3.24) was close to that of salicylic acid (3.0),<sup>41</sup> as reported by a previous study.

The  $K$  values between boronic acid and the diol compounds were determined by fluorometry using the fluorescent dye ARS.<sup>31,32,42</sup> ARS alone exhibits weak fluorescence; however, when it forms an ester bond with PBAs, it exhibits strong fluorescence. The  $K$  value between the PBA and ARS was calculated from the fluorescence intensity shift. Essentially, when a diol compound is added to an ARS/PBA solution, the PBAs and diol compounds competitively form ester bonds, and the fluorescence of the solution decreases. Thus, by analysing the decrease in fluorescence, the  $K$  value between the PBAs and diol compounds can be calculated. Reportedly, boronic acid and the diol moiety of HA form an ester bond that self-crosslinks with boronic-acid-modified HA.<sup>27–30</sup> The  $K$  value cannot be accurately calculated using BA-HA as boronic acid because the boronic acid moiety forms an ester bond not only with diol compounds but also with the diol moiety of HA. Thus, herein, 3AcAmBA was used as the boronic acid moiety instead of BA-HA. Similarly, NaSal was used instead of Sal-HA. The resulting  $K$  values are listed in Table 1. The  $K$  value for ARS increased with pH in the pH range of 5.4–7.4 ( $2440\text{--}3580 \text{ M}^{-1}$ ), beyond which it decreased up to  $666 \text{ M}^{-1}$  at pH 9.4. The  $K$  values



**Table 1** Apparent binding constants ( $K$ ) between 3AcAmBA and diol compounds at pH 7.4

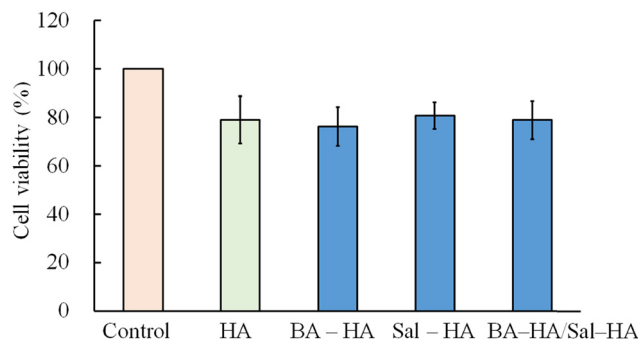
Diol	$K$ ( $M^{-1}$ )					$pK_{a-Diol}$	Predicted $pH_{K_{max}}$
	pH	5.4	6.4	7.4	8.4	9.4	
ARS		2440	3280	3580	1167	666	5.5 <sup>b</sup>
Fru		7.3	67	674	881	804	11.7 <sup>c</sup>
Glc		– <sup>a</sup>	1.8	11.5	16.0	9.5	12.1 <sup>c</sup>
NaSal		475	286	57.3	126	280	3.0 <sup>d</sup>

<sup>a</sup> The  $K$  was too low to accurately measure and could not be determined.<sup>b</sup> From ref. 6. <sup>c</sup> From ref. 55. <sup>d</sup> From ref. 41.

for Fru and Glc showed a similar pH dependence, in that the  $K$  values increased with pH except at pH 9.4 (7.3–881 and 1.8–16.0  $M^{-1}$ , respectively). In particular, the  $K$  value of Fru was 37–85 times higher than that of Glc. The behaviour of the  $K$  values in this study was similar to that of PBA previously reported.<sup>6,40</sup> These results support the effective decrease in  $G'$  upon the addition of Fru (Fig. 7e). The  $K$  value for NaSal was the highest (475  $M^{-1}$ ) at pH 5.4 and the lowest (57.3  $M^{-1}$ ) at pH 7.4. The  $K$  value of 3-fluorophenylboronic acid ( $pK_a$  8.4–8.5<sup>43</sup>) for NaSal at pH 7.4 was 166  $M^{-1}$ ; thus, the  $K$  value of 3AcAmBA for NaSal at pH 7.4 (57.3  $M^{-1}$ ) is relatively reasonable. These  $K$  values for NaSal partially explain a wide range of higher  $G'$  than that of  $G''$  at pH 4.0–8.2 (Fig. 7b). Although the  $K$  value for NaSal was as relatively higher as 280  $M^{-1}$  at pH 9.4 than that at pH 7.4, it cannot support the result that the  $G'$  values at pH 9.4 and 11.2 were much lower than those at pH 4.0–8.2 (Fig. 7b). The fluorescence properties of ARS are pH dependent,<sup>42</sup> and generally, the  $K$  value can only be measured up to at pH 8.5<sup>6,40</sup> or 8.7<sup>31</sup> even at high pH using the ARS method. Therefore, it may be inappropriate to estimate  $K$  at pH 9.4 using the ARS method. The hydroxyl groups of HA dissociate at extremely high pH (pH 12.6), destabilising the hydrogen bond network and causing a drastic decrease in viscosity.<sup>44</sup> Moreover, hyaluronan decomposes faster at pH 13, and a decrease in the average molecular weight leads to decrease in viscosity.<sup>45</sup> These physicochemical properties of HA may lead the low viscoelasticity of the BA-HA/Sal-HA system at pH > 9.4. To tune the pH dependence of the boronate-ester-cross-linked hydrogels or to increase the  $K$  value of boronate esters at physiological pH, the  $pK_a$  of PBA derivatives is often of interest.<sup>9,12</sup> There are several approaches to lower the  $pK_a$  of PBA derivatives:<sup>46,47</sup> (I) highly electron-withdrawing groups such as halogens (e.g. fluoro) and nitro groups,<sup>48</sup> (II) intra-molecular B–N<sup>49</sup> or B–O coordination bonds,<sup>50,51</sup> (III) benzoxaborole derivatives, cyclic analogues of boronic acid,<sup>7,30,52</sup> and (IV) heterocyclic boronic acids such as pyridine boronic acid.<sup>53,54</sup> However, it must be noted that the  $K$  value of boronate esters is influenced not only by the  $pK_a$  of PBA derivatives but also by the  $pK_a$  of diol compounds.<sup>40</sup> The pH at which the highest  $K$  value is achieved ( $pH_{K_{max}}$ ) is expressed using the following equation:<sup>40</sup>

$$\text{Predicted } pH_{K_{max}} = \frac{(pK_{a-BA} + pK_{a-Diol})}{2} \quad (1)$$

where  $pK_{a-BA}$  and  $pK_{a-Diol}$  represent the  $pK_a$  values of boronic acid and the diol compound, respectively. The  $pK_a$  values of ARS, Fru,

**Fig. 11** Cytocompatibility of the native HA or modified HA samples. The data represent the mean  $\pm$  standard deviation ( $n = 5$ ).

Glc, and salicylic acid have been reported in the literature as 5.5,<sup>6</sup> 11.7,<sup>55</sup> 12.1,<sup>55</sup> and 3.0,<sup>41</sup> respectively (Table 1). As the  $pK_a$  of 3AcAmBA is 8.53, the predicted  $pH_{K_{max}}$  values are 7.0, 10.1, 10.3, and 5.8 for ARS, Fru, Glc, and NaSal, respectively (Table 1). These values partly explain the pH dependence of the obtained  $K$  values.

### In vitro biocompatibility test

The biocompatibility of the injectable hydrogels is evaluated for biological applications.<sup>12,56,57</sup> MTT assay is one of the commonly used methods to evaluate cytotoxicity.<sup>12,56,58</sup> Based on previous studies,<sup>59–61</sup> A549 cells were adopted for the MTT assay in this study. The concentration of HA applied to cells was 2.0 mg  $mL^{-1}$ . The BA-HA/Sal-HA sample contained 1.0 mg  $mL^{-1}$  BA-HA and 1.0 mg  $mL^{-1}$  Sal-HA (totally 2.0 mg  $mL^{-1}$  modified HA). This concentration was lower than those for other studies on the BA-HA/Sal-HA system because a high polymer concentration increases viscoelasticity, impeding the operation of the dispenser. Moreover, in some hydrogel studies, cytocompatibility tests were performed at polymer concentrations lower than those used in rheological measurements.<sup>12,61,62</sup> The MTT assay results are shown in Fig. 11. A sample without HA was used as a control and its cell viability was normalised as 100%. The cell viabilities of native HA, BA-HA, Sal-HA and BA-HA/Sal-HA were 79.0%  $\pm$  9.8%, 76.2  $\pm$  8.1%, 80.7  $\pm$  5.4% and 78.9  $\pm$  7.8%, respectively. All HA-applied-samples showed a minor biocompatibility decrease to 76.2–80.7% in relation to the control. A similar slight decrease in biocompatibility has also been reported for some HA materials.<sup>63–65</sup> In general, native HA has high biocompatibility.<sup>61</sup> Therefore, the high biocompatibility result of native HA is reasonable. Similarly, we observed that the BA-HA/Sal-HA system exhibited high biocompatibility (78.9%), which was almost equivalent to that of native HA (79.0%).

## Conclusions

In this study, a BA-HA/Sal-HA hydrogel with injectable and self-healing properties at physiological pH was successfully prepared. Sal-HA can be prepared inexpensively *via* easy one-step synthesis. The BA-HA/Sal-HA system behaved as a sol at



pH 12.0, whereas it behaved as a gel over a wide pH range of 4.0–8.2. Moreover, the viscoelasticity of the system decreased in response to sugar at pH 7.3. Salicylic acid is a promising diol moiety for hydrogel formation *via* boronate esters for practical applications and large-scale synthesis.

## Conflicts of interest

The authors declare no competing financial interest.

## Acknowledgements

We thank Naoki Hamada for his contributions to rheological measurements.

## References

- 1 S. Correa, A. K. Grosskopf, H. Lopez Hernandez, D. Chan, A. C. Yu, L. M. Stapleton and E. A. Appel, *Chem. Rev.*, 2021, **121**, 11385–11457.
- 2 P. Bertsch, M. Diba, D. J. Mooney and S. C. G. Leeuwenburgh, *Chem. Rev.*, 2023, **123**, 834–873.
- 3 H. Montazerian, E. Davoodi, A. Baidya, S. Baghdasarian, E. Sarikhani, C. E. Meyer, R. Haghniaz, M. Badv, N. Annabi, A. Khademhosseini and P. S. Weiss, *Chem. Rev.*, 2022, **122**, 12864–12903.
- 4 M. M. Perera and N. Ayres, *Polym. Chem.*, 2020, **11**, 1410–1423.
- 5 X. Wu, Z. Li, X. X. Chen, J. S. Fossey, T. D. James and Y. B. Jiang, *Chem. Soc. Rev.*, 2013, **42**, 8032–8048.
- 6 G. Springsteen and B. Wang, *Tetrahedron*, 2002, **58**, 5291–5300.
- 7 Y. Chen, D. Diaz-Dussan, D. Wu, W. Wang, Y. Y. Peng, A. B. Asha, D. G. Hall, K. Ishihara and R. Narain, *ACS Macro Lett.*, 2018, **7**, 904–908.
- 8 M. Shan, C. Gong, B. Li and G. Wu, *Polym. Chem.*, 2017, **8**, 2997–3005.
- 9 N. Lagneau, L. Terriac, P. Tournier, J. J. Helesbeux, G. Viault, D. Séraphin, B. Halgand, F. Loll, C. Garnier, C. Jonchère, M. Rivière, A. Tessier, J. Lebreton, Y. Maugars, J. Guicheux, C. Le Visage and V. Delplace, *Biomater. Sci.*, 2023, **11**, 2033–2045.
- 10 Y. Xiang, S. Xian, R. C. Ollier, S. Yu, B. Su, I. Pramudya and M. J. Webber, *J. Controlled Release*, 2022, **348**, 601–611.
- 11 Z. Ye, Y. Xiang, T. Monroe, S. Yu, P. Dong, S. Xian and M. J. Webber, *Biomacromolecules*, 2022, **23**, 4401–4411.
- 12 T. Figueiredo, J. Jing, I. Jeacomine, J. Olsson, T. Gerfaud, J. G. Boiteau, C. Rome, C. Harris and R. Auzély-Velty, *Biomacromolecules*, 2020, **21**, 230–239.
- 13 T. Figueiredo, V. Cosenza, Y. Ogawa, I. Jeacomine, A. Vallet, S. Ortega, R. Michel, J. D. M. Olsson, T. Gerfaud, J. G. Boiteau, J. Jing, C. Harris and R. Auzély-Velty, *Soft Matter*, 2020, **16**, 3628–3641.
- 14 M. C. Roberts, M. C. Hanson, A. P. Massey, E. A. Karren and P. F. Kiser, *Adv. Mater.*, 2007, **19**, 2503–2507.
- 15 M. C. Roberts, A. Mahalingam, M. C. Hanson and P. F. Kiser, *Macromolecules*, 2008, **41**, 8832–8840.
- 16 Y. Hu, Y. Jia, S. Wang, Y. Ma, G. Huang, T. Ding, D. Feng, G. M. Genin, Z. Wei and F. Xu, *Adv. Healthcare Mater.*, 2023, **12**, 2201594.
- 17 Y. Kong, W. Shi, D. Zhang, X. Jiang, M. Kuss, B. Liu, Y. Li and B. Duan, *Appl. Mater. Today*, 2021, **24**, 101090.
- 18 E. Montanari, A. Gennari, M. Pelliccia, C. Gourmel, E. Lallana, P. Matricardi, A. J. McBain and N. Tirelli, *Macromol. Biosci.*, 2016, **16**, 1815–1823.
- 19 Z. Huang, P. Delparastan, P. Burch, J. Cheng, Y. Cao and P. B. Messersmith, *Biomater. Sci.*, 2018, **6**, 2487–2495.
- 20 J. P. Wiley, K. A. Hughes, R. J. Kaiser, E. A. Kesicki, K. P. Lund and M. L. Stolzowicz, *Bioconjugate Chem.*, 2001, **12**, 240–250.
- 21 M. L. Stolzowicz, C. Ahlem, K. A. Hughes, R. J. Kaiser, E. A. Kesicki, G. Li, K. P. Lund, S. M. Torkelson and J. P. Wiley, *Bioconjugate Chem.*, 2001, **12**, 229–239.
- 22 Y. Miyazaki, H. Matsuo, T. Fujimori, H. Takemura, S. Matsuoka, T. Okobira, K. Uezu and K. Yoshimura, *Polyhedron*, 2008, **27**, 2785–2790.
- 23 R. Miki, T. Yamaki, M. Uchida and H. Natsume, *RSC Adv.*, 2022, **12**, 6668–6675.
- 24 M. H. Kim, D. T. Nguyen and D. D. Kim, *J. Pharm. Invest.*, 2022, **52**, 397–413.
- 25 S. An, S. Choi, S. Min and S. W. Cho, *Biotechnol. Bioprocess Eng.*, 2021, **26**, 503–516.
- 26 Y. W. Ding, Z. Y. Wang, Z. W. Ren, X. W. Zhang and D. X. Wei, *Biomater. Sci.*, 2022, **10**, 3393–3409.
- 27 R. Miki, T. Yamaki, M. Uchida and H. Natsume, *Chem. Commun.*, 2023, **59**, 5114–5117.
- 28 M. Li, X. Shi, B. Yang, J. Qin, X. Han, W. Peng, Y. He, H. Mao, D. Kong and Z. Gu, *Carbohydr. Polym.*, 2022, **296**, 119953.
- 29 E. Holz and K. Rajagopal, *Macromol. Chem. Phys.*, 2020, **221**, 2000055.
- 30 T. Figueiredo, Y. Ogawa, J. Jing, V. Cosenza, I. Jeacomine, J. D. M. Olsson, T. Gerfaud, J. G. Boiteau, C. Harris and R. Auzély-Velty, *Polym. Chem.*, 2020, **11**, 3800–3811.
- 31 W. L. A. Brooks, C. C. Deng and B. S. Sumerlin, *ACS Omega*, 2018, **3**, 17863–17870.
- 32 A. Larcher, A. Lebrun, M. Smietana and D. Laurencin, *New J. Chem.*, 2018, **42**, 2815–2823.
- 33 Y. Dong, S. Chen, P. Ning, K. Lu, S. Ma, Y. Wang and S. Lü, *Polymer*, 2021, **225**, 123749.
- 34 H. Gao, C. Yu, Q. Li and X. Cao, *Carbohydr. Polym.*, 2021, **258**, 117663.
- 35 D. Tarus, E. Hachet, L. Messenger, B. Catargi, V. Ravaine and R. Auzély-Velty, *Macromol. Rapid Commun.*, 2014, **35**, 2089–2095.
- 36 S. Xian, M. A. Vandenberg, Y. Xiang, S. Yu and M. J. Webber, *ACS Biomater. Sci. Eng.*, 2022, **8**, 4873–4885.
- 37 S. H. Hong, S. Kim, J. P. Park, M. Shin, K. Kim, J. H. Ryu and H. Lee, *Biomacromolecules*, 2018, **19**, 2053–2061.
- 38 K. H. Shen, Y. Y. Yeh, T. H. Chiu, R. Wang and Y. C. Yeh, *ACS Biomater. Sci. Eng.*, 2022, **8**, 4249–4261.



- 39 M. Liu, Y. Huang, C. Tao, W. Yang, J. Chen, L. Zhu, T. Pan, R. Narain, K. Nan and Y. Chen, *Gels*, 2023, **9**, 24.
- 40 J. Yan, G. Springsteen, S. Deeter and B. Wang, *Tetrahedron*, 2004, **60**, 11205–11209.
- 41 W. L. Mock and L. A. Morsch, *Tetrahedron*, 2001, **57**, 2957–2964.
- 42 G. Springsteen and B. Wang, *Chem. Commun.*, 2001, 1608–1609.
- 43 R. Miki, T. Yamauchi, K. Kawashima, Y. Egawa and T. Seki, *Langmuir*, 2021, **37**, 3438–3445.
- 44 I. Gatej, M. Popa and M. Rinaudo, *Biomacromolecules*, 2005, **6**, 61–67.
- 45 A. Maleki, A. L. Kjøniksen and B. Nyström, *Macromol. Symp.*, 2008, **274**, 131–140.
- 46 D. Li, Y. Chen and Z. Liu, *Chem. Soc. Rev.*, 2015, **44**, 8097–8123.
- 47 W. L. A. Brooks and B. S. Sumerlin, *Chem. Rev.*, 2016, **116**, 1375–1397.
- 48 A. Matsumoto, S. Ikeda, A. Harada and K. Kataoka, *Biomacromolecules*, 2003, **4**, 1410–1416.
- 49 T. K. Kyoung, J. J. L. M. Cornelissen, R. J. M. Nolte and J. C. M. Van Hest, *J. Am. Chem. Soc.*, 2009, **131**, 13908–13909.
- 50 X. Yang, M. C. Lee, F. Sartain, X. Pan and C. R. Lowe, *Chem. – Eur. J.*, 2006, **12**, 8491–8497.
- 51 C. C. Deng, W. L. A. Brooks, K. A. Abboud and B. S. Sumerlin, *ACS Macro Lett.*, 2015, **4**, 220–224.
- 52 M. Dowlut and D. G. Hall, *J. Am. Chem. Soc.*, 2006, **128**, 4226–4227.
- 53 S. Iwatsuki, Y. Kanamitsu, H. Ohara, E. Watanabe and K. Ishihara, *J. Phys. Org. Chem.*, 2012, **25**, 760–768.
- 54 A. Matsumoto, A. J. Stephenson-Brown, T. Khan, T. Miyazawa, H. Cabral, K. Kataoka and Y. Miyahara, *Chem. Sci.*, 2017, **8**, 6165–6170.
- 55 F. Urban and P. A. Shaffer, *J. Biol. Chem.*, 1932, **94**, 697–715.
- 56 A. Pettignano, S. Grijalvo, M. Häring, R. Eritja, N. Tanchoux, F. Quignard and D. Díaz Díaz, *Chem. Commun.*, 2017, **53**, 3350–3353.
- 57 Y. Li, L. Yang, Y. Zeng, Y. Wu, Y. Wei and L. Tao, *Chem. Mater.*, 2019, **31**, 5576–5583.
- 58 W. Shi, B. Hass, M. A. Kuss, H. Zhang, S. Ryu, D. Zhang, T. Li, Y. Long Li and B. Duan, *Carbohydr. Polym.*, 2020, **233**, 115803.
- 59 J. Kurihara, M. Uchida, T. Yamaki, T. Hatanaka, T. Seki and H. Natsume, *J. Pharm. Sci. Technol., Jpn.*, 2020, **80**, 156–161.
- 60 G. T. Williams, A. C. Sedgwick, S. Sen, L. Gwynne, J. E. Gardiner, J. T. Brewster, J. R. Hiscock, T. D. James, A. T. A. Jenkins and J. L. Sessler, *Chem. Commun.*, 2020, **56**, 5516–5519.
- 61 H. Yu, Y. Liu, H. Yang, K. Peng and X. Zhang, *Macromol. Rapid Commun.*, 2016, **37**, 1723–1728.
- 62 M. Lin, P. Sun, G. Chen and M. Jiang, *Chem. Commun.*, 2014, **50**, 9779–9782.
- 63 J. H. Lee, P. Y. Kim, Y. C. Pyun, J. Park, T. W. Kang, J. S. Seo, D. H. Lee and G. Khang, *Biomater. Sci.*, 2023, **12**, 479–494.
- 64 Y. Liu, Y. Wu, H. Lin, Y. Xiao, X. Zhu, K. Zhang, Y. Fan and X. Zhang, *Carbohydr. Polym.*, 2018, **195**, 378–386.
- 65 D. G. Boeckel, R. S. A. Shinkai, M. L. Grossi and E. R. Teixeira, *Oral Surg. Oral Med. Oral Pathol. Oral Radiol.*, 2014, **117**, e423–e428.

